# Author's Accepted Manuscript


www.elsevier.com/locate/talanta

A self-calibrating logic system and oxidase-based biosensor using $Tb^{3+}$-doped carbon dots/DNA conjugates

Zi-Han Chen, Xin-Yue Han, Ling-Xue Deng, Zi-Yang Lin, Fang-Ya Mu, Shengqiang Zhang, Guoyue Shi, Min Zhang

PII: S0039-9140(18)30846-4
DOI: https://doi.org/10.1016/j.talanta.2018.08.035
Reference: TAL18956

To appear in: *Talanta*

Received date: 15 March 2018
Revised date: 6 August 2018
Accepted date: 12 August 2018

Cite this article as: Zi-Han Chen, Xin-Yue Han, Ling-Xue Deng, Zi-Yang Lin, Fang-Ya Mu, Shengqiang Zhang, Guoyue Shi and Min Zhang, A self-calibrating logic system and oxidase-based biosensor using $Tb^{3+}$-doped carbon dots/DNA conjugates, *Talanta,* https://doi.org/10.1016/j.talanta.2018.08.035

# A self-calibrating logic system and oxidase-based biosensor using $Tb^{3+}$-doped carbon dots/DNA conjugates

Zi-Han Chen, Xin-Yue Han, Ling-Xue Deng, Zi-Yang Lin, Fang-Ya Mu, Shengqiang Zhang*, Guoyue Shi, Min Zhang*

[1] Lab of Biochemical Sensing Technology, School of Chemistry and Molecular Engineering, Shanghai Key Laboratory for Urban Ecological Processes and Eco-Restoration, East China Normal University, 500 Dongchuan Road, Shanghai 200241, China.

[2] Fujian Provincial Key Laboratory of Resources and Environment Monitoring & Sustainable Management and Utilization, College of resource and chemical engineering, Sanming University, 25 Jingdong Road, Sanming, Fujian 365004, China

zhang_shengqiang@163.com

mzhang@chem.ecnu.edu.cn

*Corresponding author. Tel./fax: +86 21 54340042.



## Abstract

$Tb^{3+}$-doped carbon dots ($Tb^{3+}$@CDs) were prepared in a facile hydrothermal method by using ammonium citrate as carbon source and $Tb^{3+}$ as dopant. A 15-bp GT-rich single-strand DNA (ssDNA) was introduced to sensitize $Tb^{3+}$ via the antenna effect for generating two fluorescence signals (CDs and $Tb^{3+}$), forming a conjugate of $Tb^{3+}$@CDs/ssDNA. The ratiometric fluorescence of $Tb^{3+}$@CDs/ssDNA could be reversibly regulated by $Ag^{+}$ and Cys, in which the fluorescence peak at 546 nm of $Tb^{3+}$ could be switched to "On" or "Off" as the signal indicator while the fluorescence peak at 444 nm of CDs remained constant as the build-in reference. The proposed $Ag^{+}$/Cys-mediated reversible fluorescence changes in $Tb^{3+}$@CDs/ssDNA was also proven for the design of a self-calibrating ratiometric fluorescence logic system. By integrated with the specific reaction between $H_2O_2$ and Cys, $Tb^{3+}$@CDs/ssDNA was applied for ratiometric fluorescence detection of $H_2O_2$. More importantly, the sensing

strategy could be further successfully extended to the monitoring of $H_2O_2$-produced oxidase-related reactions, such as GOx-biocatalyzed oxidation of glucose (the limit of detection: 0.06 μM) and was well applied in rat serum compared to commercial kits. This work unveiled a novel ratiometric fluorescent design, which is cost-effective, simple to prepare and easy-to-use without chemical modification or fluorescence labeling.

**Keywords**: $Tb^{3+}$@CD/ssDNA conjuagates; Self-calibrating logic gate; Label-free ratiometric; Oxidase-based biosensor

## 1. **Introduction**

Carbon dots (CDs), as a novel generation of zero dimensional nanomaterials, has been widely applied for biochemical analysis in recent years. Due to their excellent performances such as low toxicity, cost-effectiveness, strong fluorescence emission, etc [1]. Combined with traditonal CDs, metal ion-doped CDs could provide a unique opportunity to exploit their peculiarity and broaden applications in intriguing fields [2]. For example, $Zn^{2+}$-doped carbon dots were synthesized using $Zn^{2+}$ and citric acid as the precursor via a one-pot solvothermal method that yielded excitation-independent robust yellow emission [3]. In this respect, the marriage of CDs with metal ion dopants to develop novel probes/biosensors with smart features possesses more great potential. Trivalent lanthanide ions (eg. $Tb^{3+}$) have fascinating physicochemical properties due to their unique 4f orbitals, which would make them suitable as dopants for the preparation of functional materials [4]. Lanthanide-doped nanoparticles have been widely exploited in many fields by utilizing their fascinating properties, such as upconversion fluorescence [5]. Therefore, it is highly desirable to sprout novel lanthanide-doped CDs for expanding diverse applications, such as logic systems.

$Tb^{3+}$ alone in aqueous solution could hardly generate fluorescence, because it is very poor at directly absorbing light resulting from its Laporte-forbidden f–f

transitions. However, its characteristic fluorescence can be highly sensitized by certain ligands through an efficient intermolecular energy transfer process called antenna effect [6-7]. Much attention has been actively devoted to $Tb^{3+}$ coupled with sequence-specific single-strand DNA (ssDNA) (i.e. $Tb^{3+}$/ssDNA) for the construction of various biochemical probes [8-11]. While most $Tb^{3+}$/ssDNA-based probes only shown one fluorescence signal channel toward analytes indicating that this format could be easily affected by diverse sample environment and instrumental fluctuations. To overcome weak anti-interference properties, the development of $Tb^{3+}$/ssDNA-based dual-output ratiometric fluorescent probes with self-calibrating property could be a promising approach for precise biochemical analysis in practical settings, by determining the change of fluorescence intensity ratio at two different channels.

With the above facts in mind, we herein unveiled a novel type of functional conjugates made up of $Tb^{3+}$-doped CDs ($Tb^{3+}$@CDs) and ssDNA (Scheme 1). $Tb^{3+}$@CDs could be prepared using a facile one-pot hydrothermal method, in which ammonium citrate was chosen as carbon source and $Tb^{3+}$ as dopant (Scheme 1A). Under the UV excitation, $Tb^{3+}$@CDs can be illuminated to mainly fluoresce with "blue" emission peak at 444 nm resulting from CDs. The resultant $Tb^{3+}$@CDs can readily interact with the ssDNA through both the π–π stacking of CDs with ssDNA [12] and the complex of $Tb^{3+}$ to ssDNA [8]. Thereafter, the integration of $Tb^{3+}$@CDs and ssDNA can form fluorescent conjugates (i.e., $Tb^{3+}$@CDs/ssDNA), which exhibited two major emission peaks (i.e., "blue" and "green") at 444 nm and 546 nm with excitation at 290 nm (Figure S1). In addition, it is reported that $Ag^{+}$ could greatly enhance the fluorescence of $Tb^{3+}$ sensitized by GT-rich ssDNA sequences [13-14]. Thus, the fluorescence of $Tb^{3+}$@CDs/ssDNA would be enhanced at around 546 nm ("green" emission) by $Ag^{+}$ and be constant at 444 nm ("blue" emission) (Scheme 1B). It was revealed that Cys can capture $Ag^{+}$ through the interaction between thiol groups and $Ag^{+}$ [15]. Hence, facile and label-free ratiometric fluorescent assays for $Ag^{+}$ and Cys can be constructed via a competition strategy based on $Tb^{3+}$@CDs/ssDNA, in which $Tb^{3+}$/ssDNA acted as the signal indicators and CDs was used as the build-in

reference. Also, the proposed $Ag^+$/Cys-mediated reversible fluorescence changes in $Tb^{3+}$@CDs/ssDNA enabled the design of a self-calibrating ratiometric fluorescence logic system. Moreover, it is previously reported that cysteine (Cys) can be oxidized to cystine by $H_2O_2$ [16-18], a metabolic by-product from reactions catalysed by oxidases. Considering this fact, $Tb^{3+}$@CDs/ssDNA-based ratiometric fluorescence probe would be further devised as an oxidase-based biosensor by integrated with $Ag^+$/Cys-mediated ratiometric fluorescence changes in $Tb^{3+}$@CDs/ssDNA, the $H_2O_2$-induced oxidation of Cys to cystine, and the oxidase-related biocatalytic process (Scheme 1B).

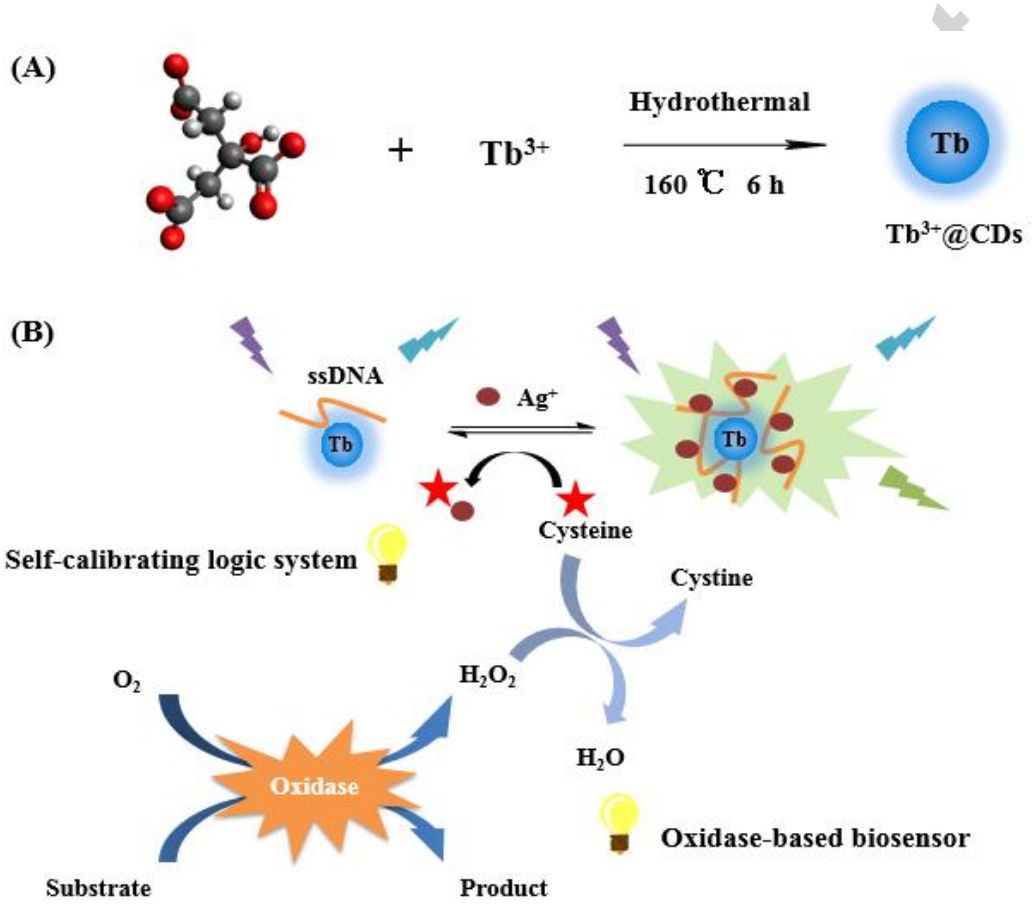


***Scheme 1.*** Schematic illustration of (A) the preparation of $Tb^{3+}$@CDs, and (B) the construction of $Tb^{3+}$@CDs/ssDNA conjugates for a self-calibrating ratiometric fluorescence logic system and oxidase-based biosensor.

## 2. Materials and Methods

### 2.1 Materials and instruments

The GT-rich oligonucleotide (5'-GGTTGGTGTGGTTGG-3') used in this study was synthesized by Sangon Biotech Co., Ltd. (Shanghai, China). Terbium (III) nitrate hexahydrate ($Tb(NO_3)_3$) was purchased from Diyang Chemical Co., Ltd. (Shanghai, China). The following reagent-grade metal salts: $Mg(NO_3)_2$, $Cu(NO_3)_2$, $Mn(Ac)_2$, $Zn(Ac)_2$, $Cr(NO_3)_3$, $Pb(NO_3)_2$, $Ni(NO_3)_2$, $Co(Ac)_2$, $Cd(NO_3)_2$, $Fe(NO_3)_3$, $Ca(Ac)_2$, $Al(NO_3)_3$, $NaNO_3$, $KNO_3$, fructose (Fru), lactose (Lac), sucrose (Suc), maltose (Mat), and galactose (Gal) were purchased from Sinopharm Chemical Reagent Co. Ltd. (Shanghai, China). L-asparagine (L-Asn), L-aspartic acid (L-Asp), L-leucine (L-Leu), L-glutamic acid (L-Glu), L-alanine (L-Ala), L-isoleucine (L-Ile), L-tyrosine (L-Tyr), L-valine (L-Val), L-threonine (L-Thr), Glycine (Gly), DL-phenylalanine (DL-Phe), L-glutamine (L-Gln), L-serine (L-Ser), L-proline (L-Pro), L-histidine (L-His), L-tryptophan (L-Trp), L-lysine (L-Lys), L-methionine (L-Met), L-arginine (L-Arg), L-cysteine (L-Cys) were purchased from Sigma-Aldrich (St. Louis, MO). Glucose oxidase (GOx) was purchased from Aladdin (Shanghai) Co., Ltd. Glucose was purchased from Qiangsheng Chemical (Jiangsu, China) Co., Ltd. Glucose assay kit (Glu Kit) was purchased from Shanghai Mind Bioengineering Co, Ltd. All the solutions were prepared in ultrapure water purified by a Milli-Q purification system (18.2 $M\Omega \cdot cm^{-1}$, Millipore Corp., Bedford, MA). Tris-HAc buffer (100 mM, pH = 7.9) was prepared by adding certain amounts of Tris in Milli-Q system and then the pH value of the buffer was adjusted by titrating with HAc. All reagents are analytical purity grade and used directly without further purification.

UV-vis absorption spectroscopy was also measured in a microplate reader (infinite M200 pro, TECAN, Switzerland) using a transparent 96-well plate (Corning, U.S.A.). Transmission electron microscope (TEM) image was recorded using a Transmission Electron Microscope (JEM-2100F, Japan) operated at 200 kV. Energy-dispersive X-ray (EDX) spectra were recorded using an S-4800 scanning electron microscope (Hitachi, Japan). The Fourier transform infrared spectroscopy (FTIR) spectra were

obtained with a Nexus 670 optical bench (Nicolet, USA). Fluorescence spectra were recorded in a microplate reader system (infinite M200 pro, TECAN, Switzerland) using a black 384-well microplate (Corning, U.S.A.). The excitation wavelength used was 290 nm for the emission spectra. A gate time of 2 ms was used for the fluorescence spectra recording.

### 2.2 Synthesis of $Tb^{3+}$-doped carbon dots ($Tb^{3+}$@CDs).

Herein, we developed a novel hydrothermal method using ammomium citrate as carbon source and $Tb^{3+}$ as dopant ion. Briefly, ammomium citrate 2.4322 g (0.01 mol) and 0.4530 g $Tb(NO_3)_3$ hexahydrate (0.001 mol) were dissolved in 80 mL Mill-Q water water followed by stirring for 30 min, and the mixture was then transfered into a 100 mL Teflon-equipped stainless steel autoclave under hydrothermal treatment at 160 °C for 6 h. After cooling down to ambient temperature, pale yellow solution was obtained. As time goes on, the as-prepared solution was changed in dark blue by degrees. The solution was then filter with 0.22 μm filtration membrane to remove large particles, and then was dialyzed against Mill-Q water through a dialysis membrane (1000 KDa) for 48 h. The purified $Tb^{3+}$@CDs were stored at room temperature for the future use.

### 2.3 Assays for $Ag^+$ using the $Tb^{3+}$@CDs/ssDNA probe.

The $Tb^{3+}$@CDs/ssDNA probe was prepared in 10 mM Tris–HAc buffer (pH 7.9), and the mixture was incubated for 10 min at room temperature. For the ratiometric fluorescence "On" detection of $Ag^+$, different concentrations of $Ag^+$ or control samples or Mill-Q water (as blank sample) were added to the $Tb^{3+}$@CDs/ssDNA probe. The final concentration of ssDNA was 5 μM. The mixture was then incubated for 10 min at room temperature. After that an aliquot of 0.1 mL mixture was placed in the black 384 well microplate to record the fluorescence spectra from 400 nm to 700 nm (excited at 290 nm, a delay time of 0 μs and a gate time of 2 ms). Selectivity and competition experiment were conducted under the same condition (40 μM $Ag^+$ and 40

μM various metal ions were used).

### 2.4 Assays for Cys using the $Tb^{3+}$@CDs/ssDNA-$Ag^{+}$ system.

The $Tb^{3+}$@CDs/ssDNA-$Ag^{+}$ system (5 μM ssDNA and 40 μM $Ag^{+}$ were used) was prepared in 10 mM Tris–HAc buffer (pH 7.9), and the mixture was incubated for 10 min at indoor temperature. For the ratiometric fluorescence "Off" detection of Cys, different concentrations of Cys or control samples or Mill-Q water (as blank sample) were added to the as-prepared sensing system. The mixture was vortexed to mix all the reagents and then incubated for 10 min at room temperature. After that an aliquot of 0.1 mL mixture was placed in the black 384 well microplate to record the fluorescence spectra. Selectivity and competition experiment were conducted under the same condition (40 μM Cys and 40 μM other amino acids were used).

### 2.5 Assays for $H_2O_2$ via reversing the Cys-mediated ratiometric fluorescence changes in the $Tb^{3+}$@CDs/ssDNA-$Ag^{+}$ system.

30 μM Cys was firstly treated with various $H_2O_2$ concentrations for 30 min in 10 mM Tris–HAc buffer (pH 7.9), and the resulting solution was then transferred to the $Tb^{3+}$@CDs/ssDNA-$Ag^{+}$ system (40 μM $Ag^{+}$ were used). The mixture was then incubated for 10 min at room temperature. After that an aliquot of 0.1 mL mixture was placed in the black 384 well microplate to record the fluorescence spectra.

### 2.6 Assays for glucose using $Tb^{3+}$@CDs/ssDNA-$Ag^{+}$-Cys system.

For glucose sensing, 10 μL of $Tb^{3+}$@CDs/ssDNA-$Ag^{+}$-Cys suspension (5 μM ssDNA, 40 μM $Ag^{+}$ and 30 μM Cys were used) were prepared previously. 10 μL of 200 U/mL glucose oxidase (GOx) solution and 10 μL Tris-HAc buffer (100 mM, pH 7.9) were mixed and then the mixture was treated with various glucose concentration of 0, 1, 2, 5, 8, 10, 15, 20, 25, 30, 40, 50, 60, 80, 100, 125, 150 μM for 30 min at 37 °C, respectively. The total volume is 100 μL. The mixture was incubated for 10 min at ambient temperature and after that an aliquot of 100 μL mixture was placed in

the black 384 well microplate to record the fluorescence spectra. Selectivity and competition experiment were conducted under the same conditions (100 μM glucose and 1 mM other saccharides were used).

**2.7 Glucose determination in serum samples from rats.**

Serum samples from healthy male rats were used to verify the practicality of this probe. The blood collecting procedures were performed in compliance with relevant laws and institutional guidelines. Serum samples were obtained after centrifuging (8000 rpm, 15 min, 4°C) fresh blood samples after standing for 2 h. High concentration of serum is unsuitable for our work because of the detection range, so the original serum samples were diluted with ultrapure water for following experiments.

**3. Result and Discussion**

We firstly constructed the $Tb^{3+}$@CDs using a facile one-pot hydrothermal method, in which ammonium citrate was chosen as carbon source and $Tb^{3+}$ as dopant (Scheme 1A). The morphology and chemical composition of purified $Tb^{3+}$@CDs were characterized by transmission electron microscopy (TEM), energy-dispersive X-ray (EDX) spectrograph and Fourier transform-infrared (FT-IR) spectrometer. $Tb^{3+}$@CDs were well dispersed in aqueous solution and a typical TEM image in Figure 1A shows that they were monodispersed and uniform with average size less than 5 nm. And there was the characteristic peak of $Tb^{3+}$ present in the EDX spectrum of $Tb^{3+}$@CDs (Figure 1B), marking that CDs were successfully doped with $Tb^{3+}$. The FT-IR spectra of the pristine CDs and $Tb^{3+}$@CDs is shown in Figure 1C and they had similar vibration shapes, in which peaks at 1400, 1589, 3143 and 3398 $cm^{-1}$ suggested the existence of C−N stretching vibrations, C=O stretching mode, N−H, and O−H, respectively. The absorption and fluorescence excitation/emission of $Tb^{3+}$@CDs were

also investigated (Figure 1D). The absorption peak of $Tb^{3+}$@CDs at 330 nm revealed the n–π* transition of the C=O bond, and the maximum excitation wavelength was recorded at 356 nm. $Tb^{3+}$@CDs could fluoresce by a wide range of excitation wavelengths from 250 nm to 400 nm (Figure S1), and showed a maximum emission peak at 444 nm (Figure 1D).

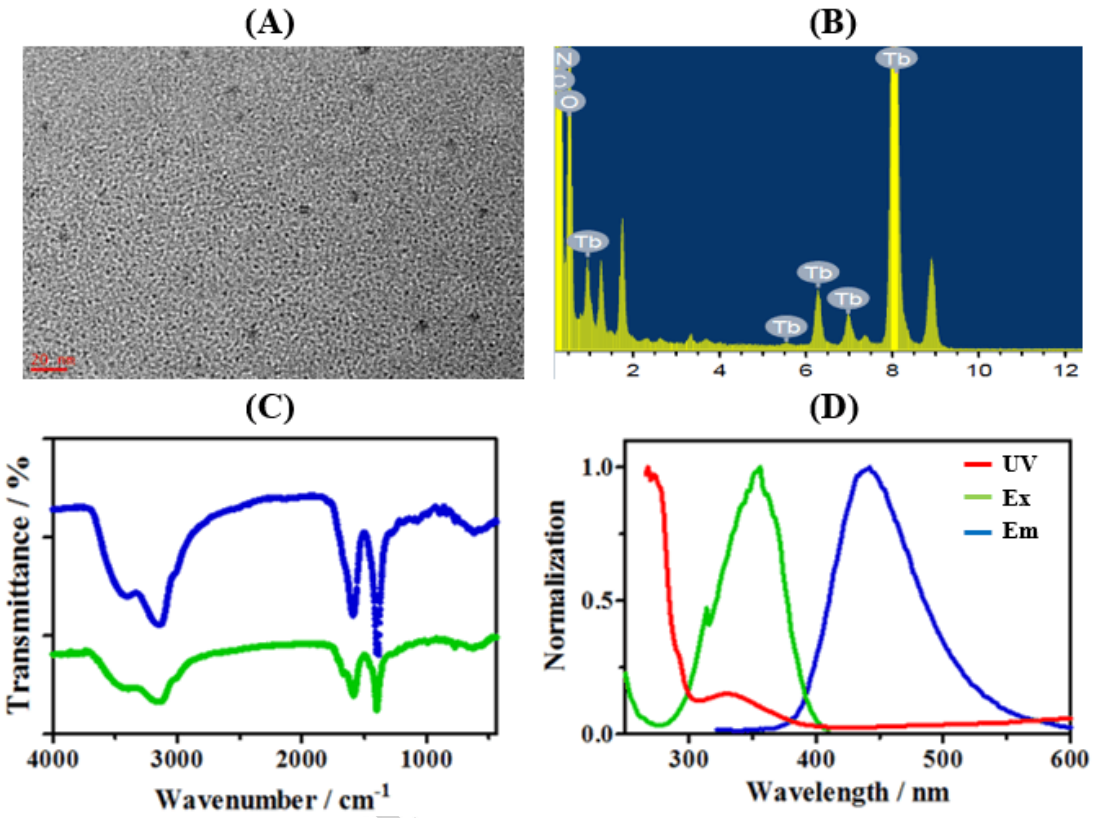


***Figure 1.*** (A) TEM image of $Tb^{3+}$@CDs; (B) EDX spectrum of $Tb^{3+}$@CDs; (C) FT-IR spectra of the pristine CDs and $Tb^{3+}$@CDs. (D) UV-vis, fluorescence excitation (Ex)/emission (Em) spectra of $Tb^{3+}$@CDs/ssDNA with a delay time of 0 μs and a gate time of 2 ms. 5 μM ssDNA was used. The resultant fluorescence emission was obtained upon excited at 356 nm.

As one proof-of-concept design, a GT-rich ssDNA was introduced into $Tb^{3+}$@CDs for the construction of $Tb^{3+}$@CDs/ssDNA conjugates. To obtain $Tb^{3+}$@CDs/ssDNA-based dual-channel ratiometric fluorescence probe, the following

emission spectra were recorded under the optimal setting (excited at 290 nm, a delay time of 0 μs, and an integration time of 2 ms) [8]. $Tb^{3+}$@CDs were firstly challenged with different concentrations of GT-rich ssDNA, and the results showed that the fluorescence of $Tb^{3+}$@CDs/ssDNA was found to be quenched at 444 nm (photo-induced transfer between CDs and ssDNA) [12] and enhanced at 546 nm (the sensitization of $Tb^{3+}$ fluorescence by GT-rich ssDNA) [8] (Figure S2). Considering both the best analytical performances (e.g. wide dynamic range) and low consumption of GT-rich ssDNA, 5 μM GT-rich ssDNA was applied to form $Tb^{3+}$@CDs/ssDNA ratiometric fluorescence conjugates for the following experiment, in which the resulting ratios of the fluorescence at 546 nm and 444 nm ($F_{546}/F_{444}$) were recorded under excitation at 290 nm.

In the absence of $Ag^{+}$, there were weak fluorescence of $Tb^{3+}$ ($F_{546}$) and high fluorescence of CDs ($F_{444}$) in the $Tb^{3+}$@CDs/ssDNA probe and it was in the close state with $F_{546}/F_{444}$ "Off". Previous studies revealed that molecular interactions between $Ag^{+}$ and G/T bases could enhance the fluorescence of $Tb^{3+}$ sensitized by ssDNA ($Tb^{3+}$/ssDNA), which was possibly due to the $Tb^{3+}$/DNA-$Ag^{+}$ ternary structures for strengthening the energy transfer (antenna effect) from G/T bases to $Tb^{3+}$ [13-14]. Based on this fact, we assumed that $Tb^{3+}$@CDs/ssDNA in the $F_{546}/F_{444}$ "Off" state could be exploited as a label-free ratiometric fluorescent probe for $Ag^{+}$. As shown in Figure 2A, the addition of increasing concentrations of $Ag^{+}$ to $Tb^{3+}$@CDs/ssDNA gave rise to the gradual fluorescence enhancement of $Tb^{3+}$ at 546 nm and the constant fluorescence of CDs at 444 nm. And the $F_{546}/F_{444}$ of $Tb^{3+}$@CDs/ssDNA was sensitive to $Ag^{+}$ in a concentration-dependent format from 0 to 40 μM (Figure 2B), that is, $Ag^{+}$ can switch the $F_{546}/F_{444}$ of $Tb^{3+}$@CDs/ssDNA from "Off" to "On" state. To illustrate the selectivity of $Ag^{+}$-induced $F_{546}/F_{444}$ response, competing metal ions including $Al^{3+}$, $Ca^{2+}$, $Cd^{2+}$, $Co^{2+}$, $Cr^{3+}$, $Cu^{2+}$, $Fe^{3+}$, $K^{+}$, $Mg^{2+}$, $Mn^{2+}$, $Na^{+}$, $Ni^{2+}$, $Pb^{2+}$, and $Zn^{2+}$ were examined under the same conditions as for $Ag^{+}$ (Figure 2C). Competition analysis for $Ag^{+}$ was also carried out with addition the same concentration of $Ag^{+}$ and various metal ions synchronously (Figure S3). Because only in the presence of $Ag^{+}$ could efficiently enhance the energy transfer from ssDNA to

$Tb^{3+}$ which would greatly increase the fluorescence intensity of $Tb^{3+}$, the results in Figure 2C clearly demonstrated that significant $F_{546}/F_{444}$ response was only observed in the case of $Ag^{+}$, while no obvious $F_{546}/F_{444}$ changes from other metal ions were measured.

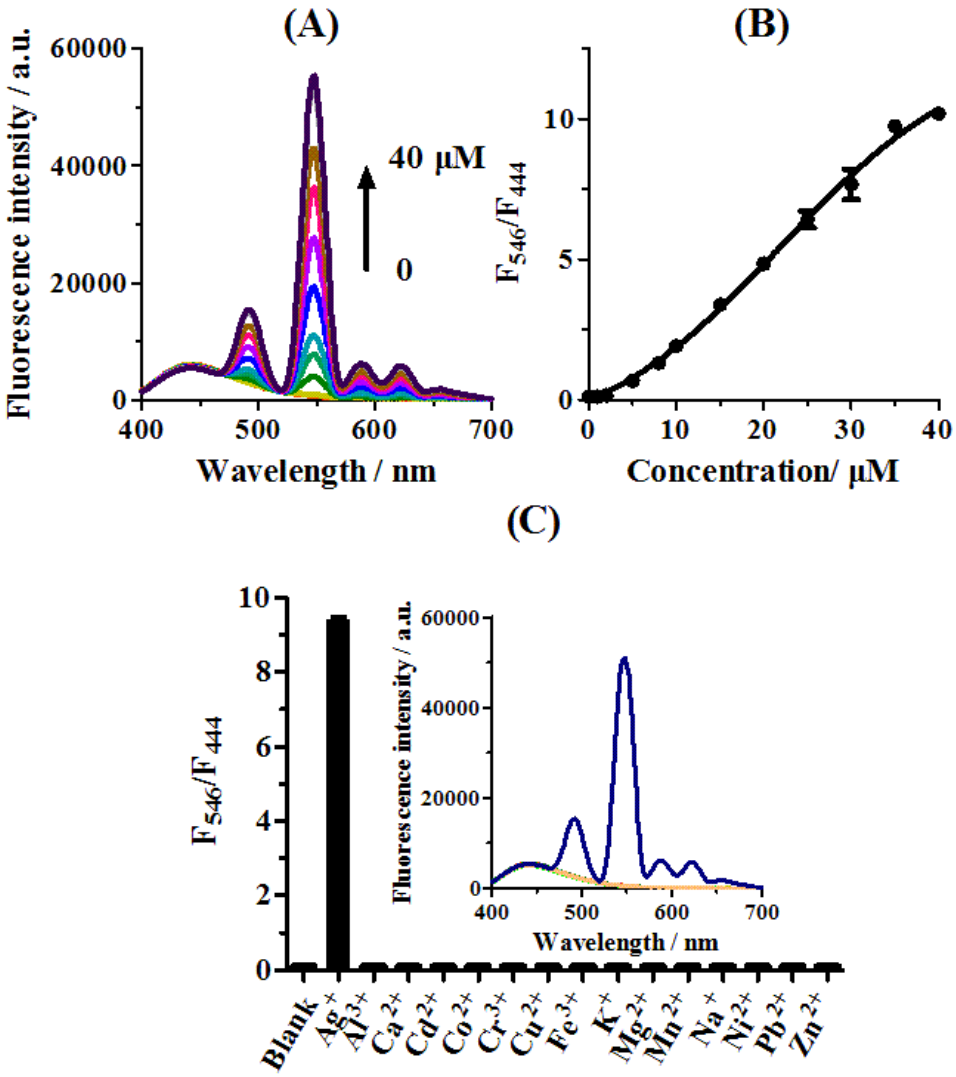


***Figure 2.*** (A) Fluorescence responses of $Tb^{3+}$@CDs/ssDNA to various concentrations of $Ag^{+}$ (0-40 μM) (5 μM ssDNA was used); (B) Plot of fluorescence ratios ($F_{546}/F_{444}$) of $Tb^{3+}$@CDs/ssDNA to the various concentration of $Ag^{+}$ indicated; (C) Bars represent the $F_{546}/F_{444}$ of $Tb^{3+}$@CDs/ssDNA to various metal ions. Inset: fluorescent spectra of $Tb^{3+}$@CDs/ssDNA to various metal ions (excited at 290 nm, a delay time of 0 μs and a gate time of 2 ms).

Upon further presence of Cys to the above system, $Ag^+$ would be removed from $Tb^{3+}$@CDs/ssDNA-$Ag^+$ and then weaken the antenna effect from ssDNA to $Tb^{3+}$, leading to the $F_{546}/F_{444}$ of $Tb^{3+}$@CDs/ssDNA from "On" to "Off" state again. Thus, the feasibility of the quantitative monitoring of Cys was further accessed based on the above $Tb^{3+}$@CDs/ssDNA-$Ag^+$ system. The results showed that a gradual $F_{546}/F_{444}$ decrease in the $Tb^{3+}$@CDs/ssDNA-$Ag^+$ system was observed upon it exposed with increasing concentrations of Cys (Figure 3A and 3B). The selectivity and competition analysis of the $Tb^{3+}$@CDs/ssDNA-$Ag^+$ system to Cys was investigated by examining its fluorescence response in the presence of various amino acids under the same conditions (Figure 3C and Figure S4). Because among 20 amino acids, only Cys have thiol group (–SH) compared to others molecular structure, and $Ag^+$ had a close affinity to –SH, in Figure 3C, 3D and Figure S4, no obvious $F_{546}/F_{444}$ decrease from other amino acids were observed, indicating the $Tb^{3+}$@CDs/ssDNA-$Ag^+$ system is suitable for specific Cys detection over other amino acids.

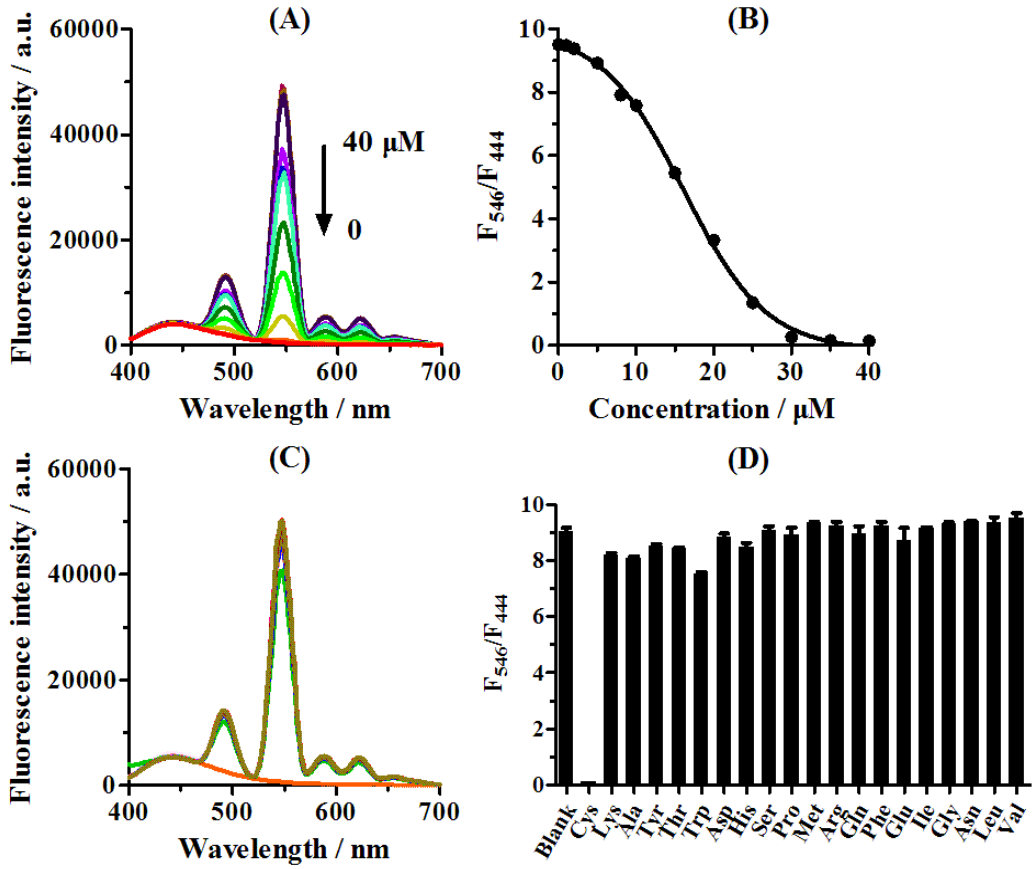


***Figure 3.*** (A) Fluorescent responses of $Tb^{3+}$@CDs/ssDNA-$Ag^{+}$ to various concentrations of Cys (0-40 μM) (5 μM ssDNA and 40 μM $Ag^{+}$ were used); (B) Plot of fluorescence ratios ($F_{546}/F_{444}$) of $Tb^{3+}$@CDs/ssDNA-$Ag^{+}$ to the various concentration of Cys indicated; (C) Fluorescent spectra of $Tb^{3+}$@CDs/ssDNA-$Ag^{+}$ to various amino acids (excited at 290 nm, a delay time of 0 μs and a gate time of 2 ms); (D) Bars represent the $F_{546}/F_{444}$ of $Tb^{3+}$@CDs/ssDNA to various amino acids.

Molecular logic systems, performing Boolean logic operations in response to chemical or physical inputs, are linchpin of modern information technology and have attracted significant recent interest [19-21]. However typical logic systems with only one signal as “IN” or “OUT” could easily be interfered by many factors [22]. Since various chemical species are employed to construct a set of logic systems, there may be cross-contamination in this process. For this issue, molecular logic systems with ratiometric responses would maximally shield signals from erroneous procedures and

be more robust in complicated environment. Inspired by the above results, we further unveiled a ratiometric fluorescence logic system with self-calibrating properties (Figure 4A). For input, the presence of $Ag^+$ or Cys was defined as 1 and their absence as 0. Ratio of the fluorescence at 546 nm and 444 nm ($F_{546}/F_{444}$) was defined as the output (1 or 0) for the logic gate. The four possible input combinations were (0, 0), (1, 0), (0, 1) and (1, 1) listed in the truth table (Figure 4B). As depicted in Figure 4B, with no input, or with Cys input alone, the output was 0; with $Ag^+$ input alone, it can facilitate the fluorescence of $Tb^{3+}$@CDs/ssDNA to enhance at 546 nm and remain unchanged at 444 nm (as the build-in reference), giving a ratiometric signal ($F_{546}/F_{444}$) as output of 1; and when the system was subjected to the two inputs together, the output was 0. The reversibility of this logic gate operation was also tested. There showed a repeated switching behavior upon alternating addition of $Ag^+$ and Cys (Figure 4C). Thus, the $Ag^+$/Cys-triggered reversible $F_{546}/F_{444}$ changes of $Tb^{3+}$@CDs/ssDNA can promise the design of a self-calibrating INHIBIT logic system based on Boolean logic, which may provide greater robustness relative to single-channel response.

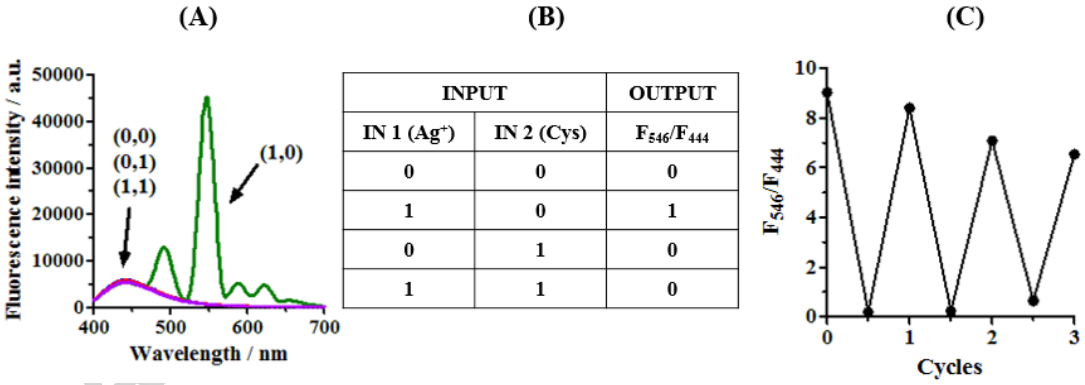


| INPUT | | OUTPUT |
|---|---|---|
| IN 1 ($Ag^+$) | IN 2 (Cys) | $F_{546}/F_{444}$ |
| 0 | 0 | 0 |
| 1 | 0 | 1 |
| 0 | 1 | 0 |
| 1 | 1 | 0 |

***Figure 4***. A ratiometric INHIBIT logic system consisting of $Tb^{3+}$@CDs/ssDNA using both $Ag^+$ and Cys as inputs (5 μM ssDNA, 40 μM $Ag^+$ and 40 μM Cys were used). (A) Fluorescent spectra of $Tb^{3+}$@CDs/ssDNA in the presence of different inputs: $Ag^+$ (0 μM) + Cys (0 μM), $Ag^+$ (40 μM) + Cys (0 μM) , $Ag^+$ (0 μM) + Cys (40 μM), and $Ag^+$ (40 μM) + Cys (40 μM) (excited at 290 nm, a delay time of 0 μs and a gate time of 2 ms) ; (B) Truth table for the INHIBIT logic system; (C) Reversible switching of the described ratiometric fluorescence logic system between the ‘‘1’’ and ‘‘0’’ states

through the addition of $Ag^+$ (40 μM) and Cys (40 μM).

As mentioned in Scheme 1B, the oxidation of Cys by $H_2O_2$ yields cystine, and the resulting disulfide reverses the Cys-mediated the $F_{546}/F_{444}$ "On-Off" shift of the $Tb^{3+}$@CDs/ssDNA-$Ag^+$ system, which can be readily applied for $H_2O_2$ sensing. Figure 5A shows the fluorescence responses of the $Tb^{3+}$@CDs/ssDNA-$Ag^+$–Cys system to various $H_2O_2$ concentrations from 0 to 150 μM, accompanying with the gradually enhancing fluorescence at 546 nm and the unchanged fluorescence at 444 nm. From Figure 5B, it can be observed that the $F_{546}/F_{444}$ "Off-On" response of the $Tb^{3+}$@CDs/ssDNA-$Ag^+$–Cys system is sensitive for monitoring of $H_2O_2$ with increasing concentrations, and the linear fitting range is from 1 to 50 μM. The successful sensitive assay to $H_2O_2$ was further extended for glucose analysis by using the $Tb^{3+}$@CDs/ssDNA-$Ag^+$–Cys system, in which glucose oxidase (GOx) can catalyze the oxidation of glucose to yield $H_2O_2$. The resulting $H_2O_2$ enable the oxidization of Cys to cystine, which can display the $F_{546}/F_{444}$ "Off-On" switch of the $Tb^{3+}$@CDs/ssDNA-$Ag^+$–Cys-GOx system (Figure 5C). The time-dependent $F_{546}/F_{444}$ responses of the $Tb^{3+}$@CDs/ssDNA-$Ag^+$–Cys-GOx system toward 100 μM glucose was investigated, and it reached a plateau within 30 min (Figure S5). After adding glucose with increasing concentrations, a gradual $F_{546}/F_{444}$ increase in the $Tb^{3+}$@CDs/ssDNA-$Ag^+$–Cys-GOx system was noticed (Figure 5D), consistent with the high content generation of $H_2O_2$ for the oxidation of Cys to cystine. The linear fitting range for glucose is from 1 to 50 μM, and the limit of detection of glucose was approximately 0.06 μM based on 3σ. Some glucose analogues were used to evaluate the selectivity and competition to glucose by our proposed method. GOx could selectively oxide glucose to gluconic acid while other glucose analogues could not be affected. Therefore, only the addition of glucose could induce a prominent $F_{546}/F_{444}$ increase of the $Tb^{3+}$@CDs/ssDNA-$Ag^+$–Cys-GOx system (Figure S6). To our

knowledge, this analytical performance can be comparable with or better than some of the reported methods as shown in Table S1, and the advantages of our proposed probe are facile to prepare without fluorescence labelling or chemical modification. Moreover, we studied the possible applicability of the $Tb^{3+}$@CDs/ssDNA-$Ag^{+}$–Cys-GOx system for the direct measurement of glucose in real samples. The unknown amount of glucose in serum samples was determined by both our method and the commercialized glucose assay kit (Table S2). Recovery of spiked known amounts of glucose to the serum samples tested by our method fully met analytical quality requirements, promising its potential practical application with great accuracy and reliability. Some of other reports have also revealed strong and practical application of $Tb^{3+}$@CDs in bioanalysis including ppGpp and ATP [23-24]. Compared to these assays, our proposed $Tb^{3+}$@CDs were via one-pot synthesized without two-step purification. And $Tb^{3+}$@CDs/ssDNA conjugates could reach multiple determination through fluorescence regulated by $Ag^{+}$/Cys and Cys-induced biochemical reactions, which exhibited its various and board applications in more environment.

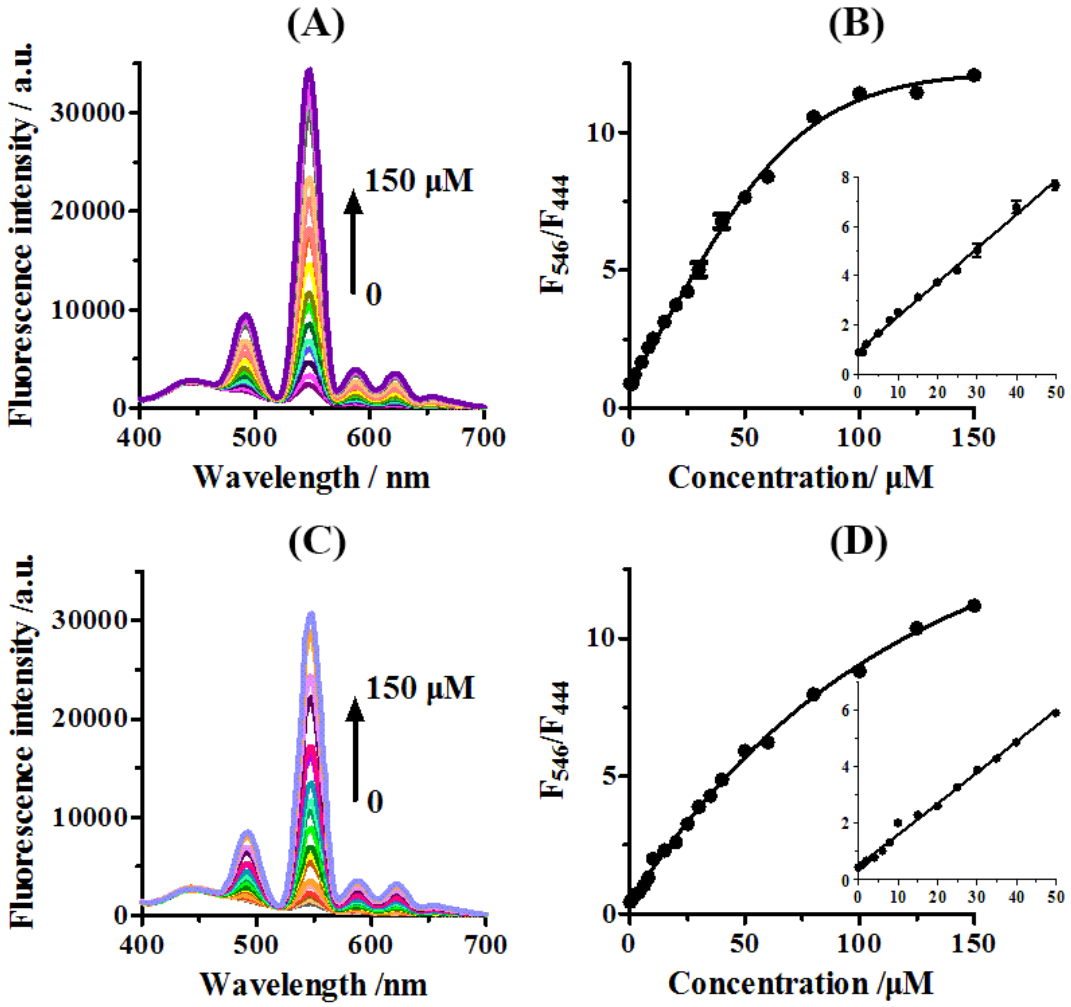


***Figure 5***. (A) Fluorescent spectra of $Tb^{3+}$@CDs/ssDNA-$Ag^{+}$-Cys to various $H_2O_2$ (0-150 μM) (5 μM ssDNA, 40 μM $Ag^{+}$ and 30 μM Cys were used); (B) Plot of the fluorescence ratio ($F_{546}/F_{444}$) vs. the concentration of $H_2O_2$ indicated; (C) Fluorescent spectra of $Tb^{3+}$@CDs/ssDNA-$Ag^{+}$-Cys to various glucose concentrations from 0-150 μM (excited at 290 nm, a delay time of 0 μs and a gate time of 2 ms); (D) Plot of the fluorescence ratio ($F_{546}/F_{444}$) vs. the concentration of glucose indicated.

## 4. Conclusion

In summary, we have proposed a novel self-calibrating ratiometric fluorescence system based on $Tb^{3+}$@CDs sensitized by ssDNA ($Tb^{3+}$@CDs/ssDNA), in which the CDs with emission at 444 nm act as the internal reference while $Tb^{3+}$/ssDNA with

emission at 546 nm serves as sensitive response indicator regulated by $Ag^+$ and Cys. The $Ag^+$/Cys-mediated "Off-On-Off" reversible fluorescence changes in the $Tb^{3+}$@CDs/ssDNA probe enabled the design of a INHIBIT logic system. This is a new concept for performance of ratiometric logic systems with self-calibration. Moreover, label-free ratiometric fluorescence assays for $Ag^+$, Cys, $H_2O_2$, and glucose in a facile, inexpensive, and mix-and-detect manner are proved based on the $F_{546}/F_{444}$ responses of the $Tb^{3+}$@CDs/ssDNA conjugates. We believe that this work will inspire and boost the progress of multifunctional $Tb^{3+}$@CDs-based biosensing platforms for various applications.

## Acknowledgments

This work was supported by the National Natural Science Foundation of China (21775044, 21675053, 21635003, 21405047), the China Scholarship Council (201706145029), the Undergraduate Innovation and Entrepreneurship Breeding Program (201710269025) funded by the Ministry of Education of China, Youth Scientific Research Project of Fujian Provincial Education Department (JAT170543, B201718), and High-level Talent Start-up Funding of Sanming University (17YG11).

## References

[1] S.Y. Lim, W. Shen, Z. Gao, Chem. Soc. Rev. 44(2015) 362–381.
[2] Q. Xu, T. Kuang, Y. Liu, L. Cai, X. Peng, T.S. Sreeprasad, P. Zhao, Z. Yue, N. Li, J. Mater. Chem. B 4(2016) 7204–7219.
[3] J. Cheng, C.F. Wang, Y. Zhang, S.Y. Yang, RSC Adv. 6(2016) 37189–37194.
[4] Z. Li, G. Wang, Y. Wang, H. Li, Angew. Chem., Int. Ed. 130(2018) 2216–2220.
[5] J. Xu, S. Zhou, D. Tu, W. Zheng, P. Huang, R. Li, Z. Chen, M. Huang, X. Chen, Chem. Sci. 7(2016) 2572–2578.
[6] H. Akiba, J. Sumaoka, M. Komiyama, ChemBiochem 10(2009) 1773–1776.
[7] S.F. Xue, L.F. Lu, Q.X. Wang, S. Zhang, M. Zhang, G. Shi, Talanta 158(2016) 208–213.
[8] M. Zhang, H.N. Le, X.Q. Jiang, B.C. Yin, B.C. Ye, Anal. Chem. 85(2013) 11665–11674.
[9] Y. Han, H. Li, Y. Hu, P. Li, H. Wang, Z, Nie, S. Yao, Anal. Chem. 87(2015) 9179–9185.
[10] W. Zhou, J. Ding, J. Liu, ChemBioChem 17(2016) 1563–1570.

[11] L. Xu, W. Zhou, J. Liu, Anal. Chim. Acta 977(2017) 44–51.
[12] H. Miao, L. Wang, Y. Zhuo, Z. Zhou, X. Yang, Biosens. Bioelectron. 86(2016) 83–89.
[13] K. Kleinke, R. Saran, J. Liu, Sensors 16(2016) 1370–1377.
[14] H. Tan, G. Tang, C. Ma, Q. Li, Anal. Chim. Acta 908(2016) 161–167.
[15] M. Zhang, H.N. Le, P. Wang, B.C. Ye, Chem. Commun. 48(2012) 10004–10006.
[16] M. Zhang, Z.b. Qu, C.M. Han, L.F. Lu, Y.Y. Li, T. Zhou, G. Shi., Chem. Commun. 50(2014) 12855–12858.
[17] L.F. Lu, Y.Y. Li, M. Zhang, G. Shi, Analyst 140(2015) 3642–3647.
[18] J.Q. Chen, S.F. Xue, Z.H. Chen, S. Zhang, G. Shi, M. Zhang, Biosens. Bioelectron. 100(2018) 526–532.
[19] J. Andreasson, U. Pischel, Chem. Rev. 44(2015) 1053–1069.
[20] M. Zhang, B.C. Ye, Chem. Commun. 48(2012) 3647–3649.
[21] Y.Y. Li, X.Q. Jiang, L.F. Lu, M. Zhang, G. Shi, Talanta 150(2016) 615–621.
[22] T. Hou, T. Zhao, W. Li, F. Li, P. Gai, J. Mat. Chem. B 5(2017) 4607–4613.
[23] B.B. Chen, M.L. Liu, L. Zhan, C.M. Li, C.Z. Huang, Anal. Chem. 90(2018) 4003-4009.
[24] M. Xu, Z. Gao, Q. Zhou, Y. Lin, M. Lu, D. Tang Biosens. Bioelectron. 86(2016) 978-984.

**Highlights:**

- A label-free ratiometric fluorescent probe has been designed using $Tb^{3+}$-doped carbon dots/ssDNA conjugates.
- $Ag^{+}$/cysteine-triggered ratiometric responses of the probe can promise the design of a novel self-calibrating logic gate.
- An oxidase-based biosensor can also be realized.

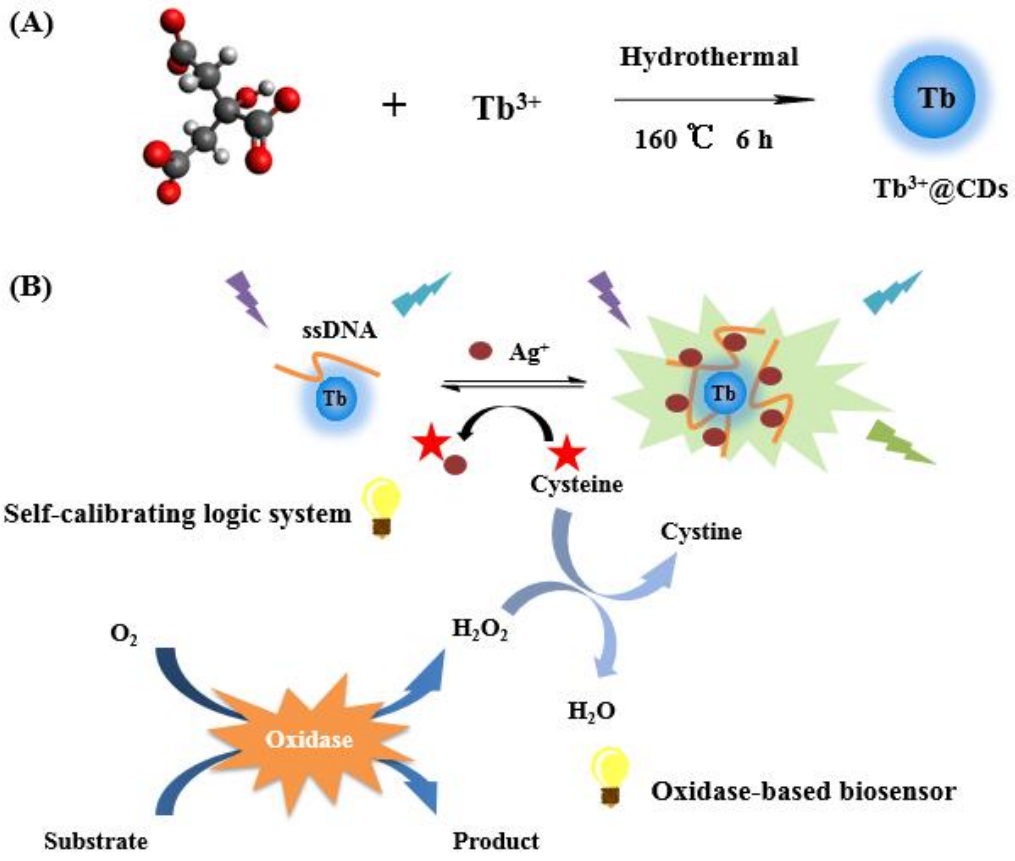


Graphical abstract